

# Time-Resolved Study of Pseudogap and Superconducting Quasiparticle Dynamics in $\text{Ca}_{0.82}\text{La}_{0.18}\text{Fe}_{1-x}\text{Ni}_x\text{As}_2$ \*

Cong-Ying Jiang(姜聪颖)<sup>1</sup>, Hai-Ying Song(宋海英)<sup>1</sup>, T. Xie(谢涛)<sup>2,3</sup>, C. Liu(刘畅)<sup>2,3</sup>, H. Q. Luo(罗会仟)<sup>2,4</sup>, S. Z. Zhao(赵时中)<sup>1</sup>, Xiu Zhang(张秀)<sup>1</sup>, X. C. Nie(聂需辰)<sup>1</sup>, Jian-Qiao Meng(孟建桥)<sup>5</sup>, Yu-Xia Duan(段玉霞)<sup>5</sup>, H. Y. Liu(刘海云)<sup>1,6\*\*</sup>, Shi-Bing Liu(刘世炳)<sup>1\*\*</sup>

<sup>1</sup>Strong-Field and Ultrafast Photonics Lab, Beijing Engineering Research Center of Laser Technology, Institute of Laser Engineering, Beijing University of Technology, Beijing 100124, China

<sup>2</sup>Beijing National Laboratory for Condensed Matter Physics, Institute of Physics, Chinese Academy of Sciences, Beijing 100190, China

<sup>3</sup>School of Physical Sciences, University of Chinese Academy of Sciences, Beijing 100190, China

<sup>4</sup>Songshan Lake Materials Laboratory, Dongguan 523808, China

<sup>5</sup>School of Physics and Electronics, Central South University, Changsha 410083, China

<sup>6</sup>Beijing Academy of Quantum Information Sciences, Beijing 100193, China

(Received 3 March 2020)

We use femtosecond time-resolved optical reflectivity to study the photoexcited quasiparticle (QP) dynamics in the iron-based 112 type superconducting (SC) samples  $\text{Ca}_{0.82}\text{La}_{0.18}\text{Fe}_{1-x}\text{Ni}_x\text{As}_2$ , with  $x = 0$  and  $0.024$ . In the parent sample, a fast and a slow relaxation emerge at temperatures below the magnetic-structure (MS) transition  $T_{\text{ms}} \approx 50$  K and the SC transition  $T_c \approx 33$  K, respectively. The latter obviously corresponds to an SC QP dynamics, which is further confirmed in the  $x = 0.024$  sample with  $T_c \approx 25$  K. The former suggests that a partial of photoexcited QP relaxation through a pseudogap (PG) channel, which is absent in the doped  $x = 0.024$  sample without the MS transition.

PACS: 74.25.Dw, 78.47.J-, 74.25.Gz, 75.30.Fv

DOI: 10.1088/0256-307X/37/6/067401

In high-temperature superconductors (HTSCs), the relation between the pseudogap (PG) state and superconductivity (SC) has been one of the major controversies. In the cuprates, the PG phase appearing above  $T_c$  in the underdoped region has been proposed to be independent/competing with SC,<sup>[1–4]</sup> or it acts as a precursor of Cooper pairs.<sup>[5–7]</sup> Very similar to the cuprates with  $\text{CuO}_2$  planes, the iron pnictide superconductors have a FeAs layer-by-layer structure. The phase diagram is more different: in RFeAsO (1111 type, with R = rare-earth element) and  $\text{AFe}_2\text{As}_2$  (122 type, A = Ba, Sr) iron pnictides, the magnetic and structure transitions in parent compounds are well suppressed when the SC phase is realized by doping,<sup>[8–12]</sup> while in LiFeAs and NaFeAs (111 type) the parent compounds are superconductors without doping.<sup>[13]</sup> More interestingly, the PG or PG-like features have been reported in all of these systems,<sup>[14–19]</sup> suggesting that study of the PG phase and its relation with SC may provide helpful understanding of the SC mechanism.

Time-resolved optical reflectivity has been proven to be an effective way of detecting the ultrafast dynamics of quasiparticles (QPs) in gapped systems. The initially photoexcited QPs first loss energy and undergo a thermalization process, then they slow down and accumulate above the gap due to a bottleneck effect. Further across-gap recombination process

occurs and is probed by a second weak pulse, resulting in the reflectivity changes in time-domain, allowing the track of QP recovery processes and analysis of gap properties. For example, in charge-density-wave (CDW) materials, this method can monitor the across-gap recovery of electron-hole pairs and resolve CDW collective excitations in  $\text{K}_{0.3}\text{MoO}_3$ .<sup>[20]</sup> In  $\text{MgB}_2$  superconducting state, the pair breaking dynamics via electron-phonon coupling has been found to dominate the transient signals right after the initial photoexcitation.<sup>[21]</sup> In cuprate superconductors, the PG and SC QP dynamics coexist below  $T_c$ , resulting in two-component relaxation in time-dependent reflectivities in  $\text{Bi}_2\text{Sr}_2\text{CaCu}_2\text{O}_{8+y}$ <sup>[22]</sup> and  $\text{Y}_{1-x}\text{Ca}_x\text{Ba}_2\text{Cu}_3\text{O}_{7-\delta}$ .<sup>[23]</sup> In iron pnictides, the PG relaxation channel has been well resolved in 111, 122 and 1111 type systems.<sup>[17,24–26]</sup> Whether the PG behavior is universal in other new type of iron pnictides is obviously an interesting question.

The recently discovered  $\text{Ca}_{1-x}\text{La}_x\text{FeAs}_2$  ( $\text{CaLa112}$ ) crystal structure has a lattice structure with FeAs layers sandwiching Ca/La layers as well as a new kind of zigzag As chains,<sup>[27]</sup> as shown in Fig. 1(a).  $\text{CaLa112}$  compounds possess structure and magnetic transitions, from a monoclinic to triclinic and from a paramagnetic (PM) to stripe antiferromagnetic (AFM) transition.<sup>[28]</sup> The replacing of Fe by Co/Ni can effectively enhance the bulk supercon-

\*Supported by the National Natural Science Foundation of China (Grant Nos. 51875009 and 51705006), the Key Project of Beijing Municipal Natural Science Foundation and Beijing Education Committee's Science and Technology Plan (Grant Nos. KZ201710005004 and KZ201810005001).

\*\*Corresponding author. Email: liuhy@baqis.ac.cn; sbliu@bjut.edu.cn

©2020 Chinese Physical Society and IOP Publishing Ltd

ductivity, and by further doping, the magnetic and structural transitions are well suppressed.<sup>[27,29,30]</sup> Its magnetic order contains both AFM and FM stripes along different directions.<sup>[29]</sup> These scenarios suggest the importance of the interactions among structure, magnetism and superconductivity in CaLa112 compounds.

In this Letter, we study QP dynamics in  $\text{Ca}_{0.82}\text{La}_{0.18}\text{Fe}_{1-x}\text{Ni}_x\text{As}_2$ , a newly discovered 112 type iron-based superconductor, using time-resolved optical reflectivity. We study the parent compound ( $x = 0$ ) with the magnetic-structure transition  $T_{\text{ms}} \approx 50$  K and the SC transition  $T_c \approx 33$  K, and a pure superconducting sample  $x = 0.024$  with only  $T_c \approx 25$  K, for comparison. We observe both the excitation and recovery dynamics of the PG and SC QPs, appearing around  $T_{\text{ms}}$  and  $T_c$  in the parent compound. The existence of SC QPs is further confirmed below  $T_c$  in the  $x = 0.024$  sample, while the PG behavior is completely absent at this doping. The coexistence of the PG and SC orders in the parent compound is supported, based on our result that the PG QP amplitude remains constant even below  $T_c$ .

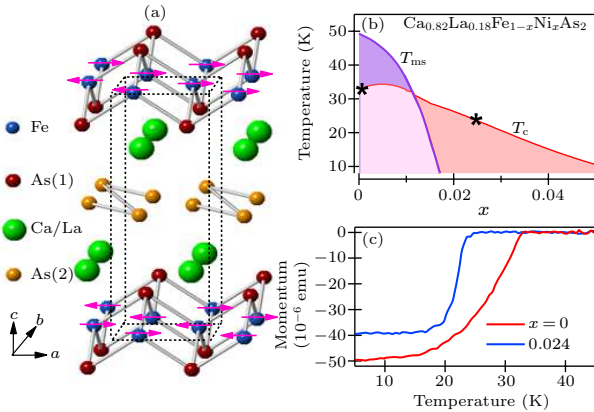


**Fig. 1.** (a) Crystal structure and magnetic order of  $\text{Ca}_{1-x}\text{La}_x\text{FeAs}_2$ . (b) The temperature versus doping ( $T$ - $x$ ) phase diagram of  $\text{Ca}_{0.82}\text{La}_{0.18}\text{Fe}_{1-x}\text{Ni}_x\text{As}_2$ .  $T_{\text{ms}}$  and  $T_c$  are the magnetic-structure and SC transitions, respectively. The black stars on the  $T_c$  curve mark the two samples at different dopings for our time-resolved measurements. (c) Superconducting transitions of the single crystals  $\text{Ca}_{0.82}\text{La}_{0.18}\text{Fe}_{1-x}\text{Ni}_x\text{As}_2$  with  $x = 0$  ( $T_c \approx 33$  K) and  $0.024$  ( $T_c \approx 25$  K) by magnetic measurements (zero-field cooled and magnetic field  $H = 10$  Oe).

In our time-resolved optical reflectivity setup, we used a Ti:sapphire amplifier system operating at a repetition rate of 1 kHz, to produce optical pulses with temporal duration of 35 fs at central wavelength of 800 nm. The sample was glued on a cryostat with a temperature sensor mounted nearby. Together with a heating loop, we could obtain a precise control of temperatures from 5 K to 300 K. Both the pump and probe beams were focused onto the  $a$ - $b$  plane of a freshly cleaved sample surface in vacuum. The spot sizes on the sample surface were about 0.4 mm (pump) and 0.2 mm (probe) in diameter, ensuring a good pump-probe overlap and all probe signals from the photoexcited volume. The probe fluence was at least an or-

der of magnitude lower than the pump beam, in order to minimize probe-induced perturbation of the system. The time delay between pump and probe pulses was realized by using a motorized delay line. With the pump beam modulated by an optical chopper, the reflected probe signal was collected by a Si-based detector and a lock-in amplifier, where the photoinduced changes in reflectivity  $\Delta R/R$  were recorded. Single crystalline  $\text{Ca}_{0.82}\text{La}_{0.18}\text{Fe}_{1-x}\text{Ni}_x\text{As}_2$  samples were grown by the self-flux method. More details of the sample growth and characterizations can be found in Refs. [29,31]. Figures 1(b) and 1(c) show the schematic phase diagram of  $\text{Ca}_{0.82}\text{La}_{0.18}\text{Fe}_{1-x}\text{Ni}_x\text{As}_2$  with different dopings and transition temperatures. We select two types of doping to study the PG and QP dynamics: the parent compound ( $x = 0$ ) that undergoes both the magnetic-structure and SC transitions, and the doped sample with  $x = 0.024$  that lies in the pure SC regime.

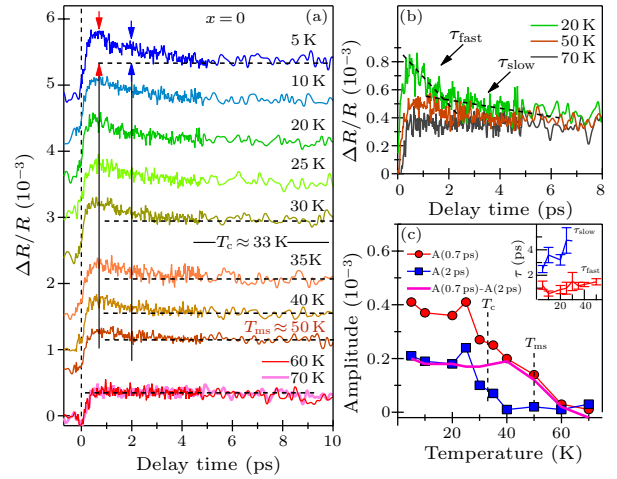


**Fig. 2.** Results of the parent compound. (a) Time-resolved reflectivity changes  $\Delta R/R$  of the parent sample ( $x = 0$ ) measured at  $F = 18 \mu\text{J}/\text{cm}^2$  from 5 to 70 K. The dashed horizontal lines represent the constant background (decay plateau) after 5 ps. The red and blue arrows denote the amplitudes of the fast and slow relaxations, peaked at 0.7 and 2 ps, respectively. (b) Selected  $\Delta R/R$  curves at 20, 50 and 70 K without offset. The dashed black lines highlight the two relaxation processes,  $\tau_{\text{fast}}$  and  $\tau_{\text{slow}}$  below  $T_c$ . (c)  $\Delta R/R$  at 0.7 and 2 ps by subtracting the background, corresponding to the amplitudes of the fast and slow components.  $A(0.7)$ - $A(2)$  is the amplitude difference between the fast and slow components, indicating that the increase of  $A(2)$  below  $T_c$  is due to the appearance of  $A(0.7)$ . The inset plots  $\tau_{\text{fast}}$  and  $\tau_{\text{slow}}$  as a function of temperature.

Figure 2(a) shows the time-resolved reflectivity changes of the parent compound at different temperatures. The curves (60 and 70 K) above  $T_{\text{ms}}$  present a constant plateau beyond the measurement regime, due to some long-lived relaxation processes such as heating diffusion. As temperature decreases, between  $T_c$  and  $T_{\text{ms}}$ , a peak feature appears at about 0.7 ps and vanishes at around 2 ps with a fast relaxation ( $\tau_{\text{fast}}$ ) in the  $\Delta R/R$  curves. More interestingly, a slow relaxation ( $\tau_{\text{slow}}$ ) in terms of an intensity uprising from 2 to 5 ps emerges in the  $\Delta R/R$  curves at around  $T_c$  and continuously increases upon temperature decreasing, giving

rise to a much clearer hump feature at 2 ps at lower temperatures. These suggest that two types of QPs appear, corresponding to two gap openings. We attribute the fast and slow relaxations to the PG and SC QP dynamics, respectively. In order to highlight the differences between phases from normal to SC states, three typical curves at 20, 50 and 70 K are plotted and normalized in Fig. 2(b), in which the fast relaxation starts appearing at  $T_{\text{ms}}$ , and it is followed by a slow relaxation in the SC phase. More detailed analyses are shown in Fig. 2(c), with extractions of the peak intensity at 0.7 ps [A(0.7)] and the hump intensity at 2 ps [A(2)] as a function of temperature. Here A(2) only appears below  $T_c$ , indicating that the slow relaxation is induced by the pure SC QP recovery/relaxation, while A(0.7) shows two abrupt changes at  $T_{\text{ms}}$  and  $T_c$ . The curve of difference A(0.7)–A(2) is reasonably used to extract the pure PG QP density, which presents no change at  $T_c$  and keeps constant at lower temperatures. In the inset of Fig. 2(c), we obtain  $\tau_{\text{fast}}$  (0.5–1.5 ps) and  $\tau_{\text{slow}}$  (2–5 ps) by fitting the relaxations using one-component ( $T_c < T < T_{\text{ms}}$ ) and two-component ( $T < T_c$ ) exponential functions with a flat background. This confirms that the fast and slow relaxation are bottlenecked QPs due to the appearing of the PG and the SC gap, respectively.

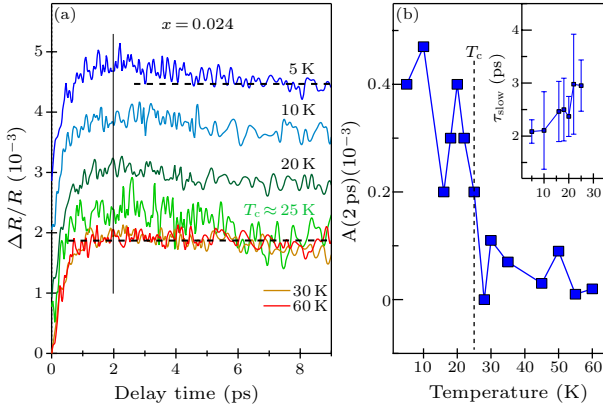


**Fig. 3.** Time-resolved results of the doped  $\text{Ca}_{0.82}\text{La}_{0.18}\text{Fe}_{1-x}\text{Ni}_x\text{As}_2$  sample with  $x = 0.024$ . (a) Temperature evolution of  $\Delta R/R$  curves. Above  $T_c$  the slow relaxation disappears, leaving only a long-lived flat plateau, as indicated by the dashed horizontal lines. (b) Temperature-dependent amplitude of the slow relaxation (peaked at 2 ps), obtained by subtracting the background. The inset plots the decay time of the slow relaxation.

Figure 3 depicts time-resolved results of the doped  $\text{Ca}_{0.82}\text{La}_{0.18}\text{Fe}_{1-x}\text{Ni}_x\text{As}_2$  with  $x = 0.024$  and  $T_c \approx 25$  K. In Fig. 3(a), again in normal state one can only see a plateau above  $T_c$ , consistent with that of the parent compound. In all curves the fast relaxation is not observed since the magnetic-structure transition is completely suppressed in this compound. In Figs. 3(a) and 3(b), only the slow relaxation robustly appears below  $T_c$  with a peak feature at 2 ps and with  $\tau_{\text{slow}}$  from 2 to 4 ps. This strongly confirms that the slow relaxation is the SC pair recovery dynamics.

The QP dynamics in gapped systems can be ana-

lytically described by the Rothwarf–Taylor model,<sup>[32]</sup> using two non-linear equations written as

$$\frac{dn_p}{dt} = \beta N_p - rn_p^2, \quad (1)$$

$$\frac{dN_p}{dt} = -\frac{1}{2}(\beta N_p - rn_p^2) - \gamma_{\text{esc}}N_p, \quad (2)$$

where  $n_p$  is the QP density/population proportional to the amplitude of the reflectivity change  $\Delta R$ , and  $N_p$  is the density of bosons populated after photoexcitation. We assume that the thermally excited densities  $n_T$  and  $N_T$  are small and neglectable at low temperatures. Here  $\beta$  is the probability of pair breaking by boson absorption and  $r$  is the rate of pair recombination with boson emission. The loss rate  $\gamma_{\text{esc}}$  refers to boson decay from photoexcited volumes. Ultra-fast photoexcitation initially breaks pairs and excites electrons to high energy levels, and in the following thermalization process the energy loss via the emission of bosons and electron scattering. The emitted high frequency bosons, which have higher energy than gaps, have chances to be reabsorbed and further excite more electron QPs, meaning a large number of  $N_p$ ,  $\beta N_p > rn_p^2$  and  $dn_p/dt > 0$ . Therefore density increases of the excited PG and SC QPs appear, corresponding to additional rising edges in  $\Delta R/R$  curves. From our experimental results, the PG QP excitation dynamics occurs from  $\sim 0$  to  $\sim 0.7$  ps below  $T_{\text{ms}}$  and the SC QP excitation takes part in the dynamics from  $\sim 0$  to  $\sim 2$  ps below  $T_c$ . In the following recombination/recovery process, with the loss of high frequency bosons (either escape from photoexcited volume or decay into low energy bosons),  $N_p$  effectively decreases to generate  $dn_p/dt < 0$ , and in this sense, recovery to equilibrium dominates the QP dynamics giving rise to decays in  $\Delta R/R$ .

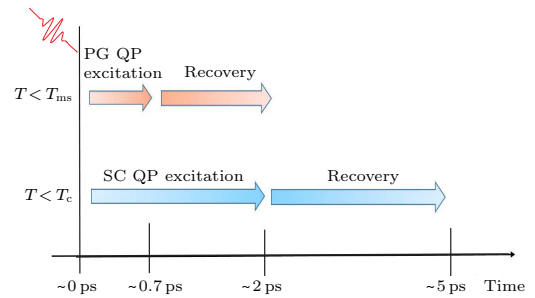


**Fig. 4.** A simple picture for the transient PG and SC QP dynamics in time domain. Below  $T_{\text{ms}}$ , the excitation of PG QP occurs from photoexcitation to 0.7 ps, while from 0.7 to 2 ps the PG QP recovery dominates the transient dynamics in terms of the fast relaxation. In the SC phase, SC QP gets excited from the initial photoexcitation to 2 ps, while the SC pair recovery plays a major role after 2 ps, giving rise to the slow relaxation. In the parent compound the PG QP dynamics appears below  $T_{\text{ms}}$  and coexists with the SC QP dynamics below  $T_c$ , while the latter only exists in the SC phase in the doped sample ( $x = 0.024$ ).

As shown in Fig. 4, a possible schematic illustration is proposed for the dynamics in different phases. In the parent sample, the PG QPs are continuously

excited up to  $\sim 0.7$  ps after the initial photoexcitation between  $T_{ms}$  and  $T_c$ , and recover from  $\sim 0.7$  to  $\sim 2$  ps. With the SC gap opening below  $T_c$ , a new bottleneck is introduced and the SC QP excitation ( $\sim 0$  to  $\sim 2$  ps) and recovery ( $\sim 2$  to  $\sim 5$  ps) are well found.

In summary, our time-resolved results on  $\text{Ca}_{0.82}\text{La}_{0.18}\text{Fe}_{1-x}\text{Ni}_x\text{As}_2$  reveal the emergence of the PG QP dynamics around  $T_{ms}$ , which coexists with the SC QP below  $T_c$  in the parent compound. Upon doping with  $x = 0.024$ , the PG channel is suppressed, leaving only the SC QP dynamics in the pure SC phase. The PG QP dynamics from our results is more or less consistent with that in other iron-based superconductors by time-resolved reflectivities,<sup>[17,24–26]</sup> indicating an universal PG physics among these materials.

## References

- [1] Tanaka K, Lee W S, Lu D H, Fujimori A, Fujii T, Risdiana, Terasaki I, Scalapino D J, Devereaux T P, Hussain Z and Shen Z X 2006 *Science* **314** 1910
- [2] Lee W S, Vishik I M, Tanaka K, Lu D H, Sasagawa T, Nagaosa N, Devereaux T P, Hussain Z and Shen Z X 2007 *Nature* **450** 81
- [3] Kondo T, Khasanov R, Takeuchi T, Schmalian J and Kaminski A 2009 *Nature* **457** 296
- [4] Hashimoto M, Nowadnick E A, He R H, Vishik I M, Moritz B, He Y, Tanaka K, Moore R G, Lu D H, Yoshida Y, Ishikado M, Sasagawa T, Fujita K, Ishida S, Uchida S, Eisaki H, Hussain Z, Devereaux T P and Shen Z X 2015 *Nat. Mater.* **14** 37
- [5] Emery V J and Kivelson S A 1995 *Nature* **374** 434
- [6] Kanigel A, Chatterjee U, Randeria M, Norman M R, Souma S, Shi M, Li Z Z, Raffy H and Campuzano J C 2007 *Phys. Rev. Lett.* **99** 157001
- [7] Meng J Q, Zhang W T, Liu G D, Zhao L, Liu H Y, Jia X W, Lu W, Dong X L, Wang G L, Zhang H B, Zhou Y, Zhu Y, Wang X Y, Zhao Z X, Xu Z Y, Chen C T and Zhou X J 2009 *Phys. Rev. B* **79** 024514
- [8] Kamihara Y, Watanabe T, Hirano M and Hosono H 2008 *J. Am. Chem. Soc.* **130** 3296
- [9] Ren Z A, Lu W, Yang J, Yi W, Shen X L, Li Z C, Che G C, Dong X L, Sun L L, Zhou F and Zhao Z X 2008 *Chin. Phys. Lett.* **25** 2215
- [10] de la Cruz C, Huang Q, Lynn J W, Li J Y, Ratcliff W, Zarestky J L, Mook H A, Chen G F, Luo J L, Wang N L and Dai P C 2008 *Nature* **453** 899
- [11] Rotter M, Tegel M and Johrendt D 2008 *Phys. Rev. Lett.* **101** 107006
- [12] Chen G F, Li Z, Li G, Hu W Z, Dong J, Zhou J, Zhang X D, Zheng P, Wang N L and Luo J L 2008 *Chin. Phys. Lett.* **25** 3403
- [13] Chu C W, Chen F, Gooch M, Guloy A M, Lorenz B, Lv B, Sasmal K, Tang Z J, Tapp J H and Xue Y Y 2009 *Physica C* **469** 326
- [14] Ahilan K, Ning F L, Imai T, Sefat A S, Jin R, McGuire M A, Sales B C and Mandrus D 2008 *Phys. Rev. B* **78** 100501
- [15] Xu Y M, Richard P, Nakayama K, Kawahara T, Sekiba Y, Qian T, Neupane M, Souma S, Sato T, Takahashi T, Luo H Q, Wen H H, Chen G F, Wang N L, Wang Z, Fang Z, Dai X and Ding H 2011 *Nat. Commun.* **2** 392
- [16] Zhao L, Liu H Y, Zhang W T, Meng J Q, Jia X W, Liu G D, Dong X L, Chen G F, Luo J L, Wang N L, Lu W, Wang G L, Zhou Y, Zhu Y, Wang X Y, Xu Z Y, Chen C T and Zhou X J 2008 *Chin. Phys. Lett.* **25** 4402
- [17] Lin K H, Wang K J, Chung C C, Wen Y C, Tsai D H, Wu Y R, Hsieh Y T, Wang M J, Lv B, Chu C W and Wu M K 2014 *Phys. Rev. B* **90** 174502
- [18] Jia X W, Liu H Y, Zhang W T, Zhao L, Meng J Q, Liu G D, Dong X L, Wu G, Liu R H, Chen X H, Ren Z A, Yi W, Che G C, Chen G F, Wang N L, Wang G L, Zhou Y, Zhu Y, Wang X Y, Zhao Z X, Xu Z Y, Chen C T and Zhou X J 2008 *Chin. Phys. Lett.* **25** 3765
- [19] Liu H Y, Jia X W, Zhang W T, Zhao L, Meng J Q, Liu G D, Dong X L, Wu G, Liu R H, Chen X H, Ren Z A, Yi W, Che G C, Chen G F, Wang N L, Wang G L, Zhou Y, Zhu Y, Wang X Y, Zhao Z X, Xu Z Y, Chen C T and Zhou X J 2008 *Chin. Phys. Lett.* **25** 3761
- [20] Demsar J, Biljaković K and Mihailović D 1999 *Phys. Rev. Lett.* **83** 800
- [21] Demsar J, Averitt R D, Taylor A J, Kabanov V V, Kang W N, Kim H J, Choi E M and Lee S I 2003 *Phys. Rev. Lett.* **91** 267002
- [22] Liu Y H, Toda Y, Shimatake K, Momono N, Oda M and Ido M 2008 *Phys. Rev. Lett.* **101** 137003
- [23] Demsar J, Podobnik B, Kabanov V V, Wolf T and Mihailović D 1999 *Phys. Rev. Lett.* **82** 4918
- [24] Chia E E M, Talbayev D, Zhu J X, Yuan H Q, Park T, Thompson J D, Panagopoulos C, Chen G F, Luo J L, Wang N L and Taylor A J 2010 *Phys. Rev. Lett.* **104** 027003
- [25] Mertelj T, Kabanov V V, Gadermaier C, Zhigadlo N D, Katrych S, Karpinski J and Mihailović D 2009 *Phys. Rev. Lett.* **102** 117002
- [26] Mertelj T, Kusar P, Kabanov V V, Stojchevska L, Zhigadlo N D, Katrych S, Bukowski Z, Karpinski J, Weyeneth S and Mihailović D 2010 *Phys. Rev. B* **81** 224504
- [27] Liu X, Liu D F, Zhao L, Guo Q, Mu Q G, Chen D Y, Shen Bing, Yi H M, Huang J W, He J F, Peng Y Y, Liu Y, He S L, Liu G D, Dong X L, Zhang J, Chen C T, Xu Z Y, Ren Z A and Zhou X J 2013 *Chin. Phys. Lett.* **30** 127402
- [28] Jiang S, Liu C, Cao H B, Birol T, Allred J M, Tian W, Liu L, Cho K, Krogstad M J, Ma J, Taddei K M, Tanatar M A, Hoesch M, Prozorov R, Rosenkranz S, Uemura Y J, Kotliar G and Ni N 2016 *Phys. Rev. B* **93** 054522
- [29] Xie T, Gong D L, Zhang W, Gu Y H, Huesges Z, Chen D F, Liu Y T, Hao L J, Meng S Q, Lu Z L, Li S L and Luo H Q 2017 *Supercond. Sci. Technol.* **30** 095002
- [30] Jiang S, Liu L, Schütt M, Hallas A M, Shen B, Tian W, Emmanouilidou E, Shi A, Luke G M, Uemura Y J, Fernandes R M and Ni N 2016 *Phys. Rev. B* **93** 174513
- [31] Xie T, Gong D L, Ghosh H, Ghosh A, Soda M, Masuda T, Itoh S, Bourdarot F, Regnault L P, Danilkin S, Li S L and Luo H Q 2018 *Phys. Rev. Lett.* **120** 137001
- [32] Rothwarf A and Taylor B N 1967 *Phys. Rev. Lett.* **19** 27